Polymer 50 (2009) 5181–5191

Contents lists available at ScienceDirect

Polymer

journal homepage: www.elsevier.com/locate/polymer

Synthesis of block copolymers for surface functionalization with stimuli-responsive macromolecules

Eva Berndt, Mathias Ulbricht*

Lehrstuhl für Technische Chemie II, Universität Duisburg-Essen, 45141 Essen, Germany

ARTICLE INFO

Article history:
Received 14 July 2009
Received in revised form
28 August 2009
Accepted 2 September 2009
Available online 18 September 2009

Keywords:
Atom transfer radical polymerization (ATRP)
Self-assembly
Stimuli-responsive polymers

ABSTRACT

Using block copolymers with poly(*n*-butyl acrylate) (PBA) as anchor block being capable to tether the temperature-responsive block poly(*N*-isopropylacrylamide) (PNIPAAm) to the surface, polysulfone (PSf) films were functionalized applying an adsorption/surface entrapment process. Homo and block copolymer synthesis was investigated applying atom transfer radical polymerization (ATRP) using tris(2-(dimethylamino)ethyl)amine (Me_6TREN), CuCl and *N*,*N*-dimethylformamide (DMF). On basis of the determined critical micelle concentration of the block copolymers, surface functionalization of PSf was performed from an aqueous solution containing 25 vol% dimethylacetamide. These functionalized surfaces exhibit reversible temperature dependent properties due to the lower critical solution temperature (LCST) of PNIPAAm as can be proven by contact angle measurement. Furthermore, the beneficial effect of the PBA block with adjusted molecular weight on the stability of these coatings was proven. This surface functionalization method has various potential applications and the resulting surfaces are anticipated to exhibit actively triggerable 'chaotic' properties as basis of an efficient anti-biofouling strategy.

1. Introduction

Most surfaces, either biological or artificial, when exposed to natural water soon get covered with organic compounds, microorganisms and their metabolites. Those assemblages are the major survival strategy of the organisms involved: biofilms provide an increased concentration of nutrients, possibilities of communication with respect to the local density of population and subsequent coordination of gene expression and thereby an effective shelter from desiccation or environmental changes, predators and toxins [1]. The matrix in which the microorganisms are immobilized contributes 50–90% [2] of the total organic carbon of biofilms and consists of secreted polysaccharides, proteins, nucleic acids, (phospho)lipids and other polymeric biosubstances summarized as extracellular polymeric substances (EPS) [3]. They are mainly responsible for the structural and functional integrity of biofilms and are considered as the key components that determine their physico-chemical and biological properties. Additionally they are said to play a crucial role in the initial step during colonization of surfaces [3].

While biofilms are advantageous to microorganisms they can have a great negative impact on lifetime and operation mode of manufactured devices. This fact is commonly referred to as biofouling. For example fuel consumption of ships is increased due to the additional friction resistance of colonized ship hulls caused by the viscoelasticity and roughness of a biofilm. However, increased costs of operation and maintenance are not the only consequences of biofouling. Contamination of drinking water or food with bacteria results in spoilage or diseases and is caused by biofouling in water distribution systems and food processing equipment. Especially in the medical field the formation of biofilms on devices like catheters and implants frequently constitutes a reason for device failure or infections [4].

As organotin compounds were recently banned most common commercially used techniques to control biofouling are based on paints which contain copper and/or organic biocides [5]. Those self-polishing surfaces release antimicrobial agents into the environment and these substances accumulate. This may cause irreversible damage to the ecosystem. Additionally this approach suffers from the problem of providing perfect conditions for resistance development to the released toxic compound [6]. Therefore, recently a strong interest in the understanding of the factors contributing to biofilm formation evolved [7]. Based on the obtained results efforts were made in the development of environmentally friendly antifouling coatings. Many of the approaches try to reduce the attractive interaction between microorganisms and the surface by optimizing the physico-chemical surface properties of the material. For example non-sticky coatings based on organosilicon

* Corresponding author. Tel.: +49 201 183 3151; fax: +49 201 183 3147.
E-mail address: mathias.ulbricht@uni-due.de (M. Ulbricht).

0032-3861/$ – see front matter © 2009 Elsevier Ltd. All rights reserved.
doi:10.1016/j.polymer.2009.09.009

compounds, so called fouling-release coatings, significantly reduce the degree of interaction so that the temporary bond formed upon contact can be broken by the weight of the fouling layer or by the motion of, e.g. a ship through the water, and the formed biofilm is released [5]. The major contributing mechanism is a surface with low surface free energy [8,9]. Another promising approach is based on polymer brushes usually composed of poly(ethylene glycol) (PEG). Those brushes are called fouling-resistant as they very much reduce the attachment of biomacromolecules and bacteria [10,11].

Even more sophisticated concepts were presented combining different approaches and avoiding development of resistance by coatings which are able to change their surface properties. With the use of multifunctional amphiphilic copolymers a heterogeneous surface can be obtained which shows interfacial adaptation when a microorganism tries to adhere. Wooley et al. [12] and Ober et al. [13] presented surfaces based on this concept. Nevertheless, microorganisms show a pronounced ability of adaptation and it is quite probable that there are strains that might also adhere to those surfaces with changing properties. This problem might be solved by surfaces which change their properties continuously but independently of the environment. Those surfaces avoid adaptation of microorganisms, because they convey contradictory signals about their nature to the approaching microorganisms. Such system should exhibit anti-biofouling activity against a broad range of microorganisms. Lopez et al. proposed stimuli-responsive polymers which can be triggered by an external stimulus [14]. Poly(*N*-isopropylacrylamide) (PNIPAAm) exhibits a lower critical solution temperature (LCST) at 32 °C and thereby provides the possibility of changing surface properties by temperature. Based on results of Okano et al. [15] and Ito et al. [16] who showed that cells detach from surfaces modified by PNIPAAm, Lopez et al. studied different coatings containing this stimuli-responsive polymer [14,17,18]. They could prove the detachment of 90% of already adsorbed microorganisms by thermally switching PNIPAAm.

Herein we present a method how to prepare stable, switchable coatings based on PNIPAAm by using block copolymer structures. The temperature-responsive polymer PNIPAAm is linked to a binder polymer which serves as an anchor during adsorption to the substrate surface [19] to firmly tether the active component in a conformation enabling maximum interaction with the environment. For that purpose poly(*n*-butyl acrylate) (PBA) was chosen as anchor block as it exhibits similar hydrophobic properties like polysulfone (PSf) onto which the block copolymer should be adsorbed from aqueous solutions (Fig. 1).

The synthesis of amphiphilic block copolymers containing *n*- or *tert*-butyl(meth)acrylate and *N*-isopropylacrylamide has been rarely described in literature and, if so, mainly with relevance to drug delivery systems. Okano et al. presented the preparation of poly(NIPAAm-*b*-BMA) by coupling hydroxyl-semitelechelic PNIPAAm with carboxylic-semitelechelic PBMA both synthesized via the technique of telomerization [20]. Due to the broad development of controlled/living polymerization techniques in recent years the synthetic access to polymer architectures such as block copolymers has grown rapidly [21]. Using either reversible addition-fragmentation chain transfer (RAFT) polymerization [22], nitroxide mediated radical polymerization (NMRP) [23] or atom transfer radical polymerization (ATRP) [24,25] the synthesis of poly(NIPAAm-*b*-B(M)A) has been presented. It should be noted that the poly(NIPAAm-*b*-*tert*-BMA) synthesized by ATRP had then been hydrolysed and the properties of the carboxylic acid copolymer had been studied [24,25]. Due to the thermal and photochemical stability of the resulting end groups and the easy commercial availability of reagents for ATRP, compared to the other two living polymerization techniques, the method of ATRP was chosen in this work for synthesis of block copolymers containing PNIPAAm and PBA.

Considering the properties of such block copolymers in solution surface functionalizations were performed via adsorption. Although this 'grafting-to' method is providing only limited grafting densities, the obtained surface modification of PSf layers was sufficient to clearly show a switching effect using contact angle measurements. Additionally, the long term stability of such layers was analysed in comparison to a homo PNIPAAm of comparable molecular weight.

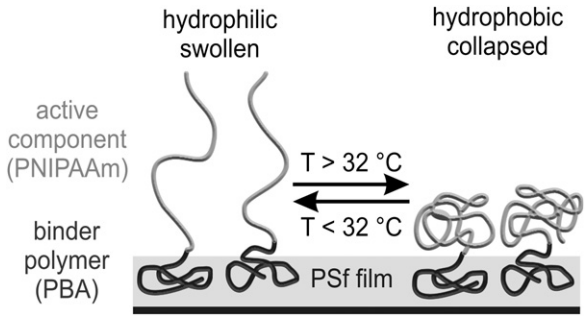

Fig. 1. Schematic concept of surface functionalization by a block copolymer composed of a temperature-switchable functional block and an anchor block.

2. Experimental section

2.1. Materials

N-Isopropylacrylamide (Acros Organics, 99%, stabilized) was recrystallized twice from *n*-hexane (Acros, p.a.), dried in vacuum and stored at 4 °C. *n*-Butyl acrylate (Fluka, ≥99%, stabilized) was dried over CaH_2 (Fluka, ≥97%), distilled under reduced pressure and stored under argon at 4 °C. Tris(2-(dimethylamino)ethyl)amine (Me_6TREN) was synthesized according to the literature [26]. Ethyl 2-chloropropionate (EClP, 97%) and CuBr (99.999%) from Aldrich, CuCl from Acros Organics (99.99%), *N*,*N*-dimethylformamide (DMF) from Normapur (p.a.), ethyl α-bromoisobutyrate (EBriB, ≥97.0%), *N*,*N*,*N*′,*N*′,*N*′-pentamethyldiethylenetriamine (PMDETA, ≥98%), dodecane (≥95%) and dimethylacetamide (DMAc) from Fluka (>98%), methanol from Fisher Scientific (p.a.) and *n*-heptane from AppliChem (p.a.) were used as received. Column isolation was performed using activated neutral aluminum oxide from Acros Organics. Polysulfone (PSf) Udel P-3500 was purchased from Amoco Chemical Belgium N.V. Silicon wafers ($9 \times 9\ mm^2$) were used from SilChem. For production of ultrapure water a Milli-Q system from Millipore was used to result in Milli-Q water with a conductivity of 18 MΩ.

2.2. Synthesis

2.2.1. General procedure for polymerization of NIPAAm

A three neck flask equipped with a stir bar was charged with NIPAAm (13.24 g, 0.117 mol, c(NIPAAm) = 3.9 mol/L), Me_6TREN (2 equiv) and DMF (30 mL). While degassing with argon for 30 min the solution was immersed in an oil bath with 25 °C to guarantee room temperature conditions. The addition of CuCl (2 equiv) caused a reddish brown precipitate which did not dissolve after additional 10 min of degassing with argon. The polymerization was started by adding the degassed initiator EClP (1 equiv), and the color slowly turned to dark green. Aliquots of 3 mL were removed at regular intervals and quenched by addition of THF. The samples were passed through a short column of aluminum oxide in order to remove the catalyst.

Conversion was determined using three different techniques: 1. the relative intensities of the ^{1}H-NMR peaks at 5.6–5.5 ppm for the

residual monomer and at 4.1–3.6 ppm for the monomer and polymer which overlap were compared; 2. the integrals of the polymer signal determined via SEC were related to the corresponding monomer signal; 3. for a gravimetric determination of the yield a defined amount of the polymer/monomer mixture was precipitated after column isolation in diethyl ether and dried over night. The obtained weight was corrected for residual monomer determined by ^{1}H-NMR spectroscopy and was compared to the solid content of this solution.

2.2.2. General procedure for polymerization of BA

BA (16.68 mL, 0.117 mol, c(BA = 3.58 mol/L)), DMF (30 mL), Me_6TREN (2 equiv) and dodecane (2.66 mL, 0.0117 mol) as internal standard for GC were introduced to a three neck flask equipped with a stir bar. The solution was degassed for 30 min and CuCl (2 equiv) was added to give a reddish brown precipitate. After degassing for another 10 min the polymerization was started by adding degassed initiator (1 equiv). Immediately, an aliquot of 3 mL was removed for analysis at start of reaction ($t = 0$), and the flask was immersed in a preheated oil bath at 70 °C. Samples of 3 mL were taken under argon flow at regular intervals to follow the kinetics. The polymerization was stopped by addition of THF and the conversion was determined using data from gas chromatography and the following equation:

$$x_p = 1 - (A_t/A_0) \quad (1)$$

where A_t and A_0 are the ratios of the peak integrals for monomer and dodecane at time t and $t = 0$ [27]. Each integral represented the average value of at least three measurements.

2.2.3. General procedure for synthesis of block copolymers

Ratios of monomer, initiator, ligand, CuCl as well as concentrations in DMF and temperatures were used as described above for the general polymerization procedures.

A three neck flask equipped with a stir bar was charged with the monomer (either BA or NIPAAm, final concentrations: c(BA) = 3.58 mol/L, c(NIPAAm) = 3.9 mol/L), Me_6TREN (2 equiv) and DMF and degassed with argon for 30 min. At the same time the macroinitiator (either PNIPAAm or PBA, respectively, obtained via ATRP as described above) (1 equiv) was dissolved in DMF and the solution was degassed for 30 min. The CuCl (2 equiv) was added to the monomer solution, and the complex was formed for another 10 min. The macroinitiator was added via a syringe, and the flask was placed in a preheated oil bath (70 °C or 25 °C). For time resolved polymerizations the procedures described above were used. For large scale experiments the polymerization was stopped by addition of THF and the solution was filtered through an aluminum oxide column. The resulting block copolymer was precipitated in MeOH:water 1:1 in a 20 fold excess. The filtered product was dried in an oven over night. For the polymerizations with PBA as macroinitiator the resulting product was precipitated once again in heptane to give the pure block copolymer without contamination by unreacted (“dead”) macroinitiator.

2.2.4. Preparation of substrate polymer films and surface functionalization via adsorption/surface entrapment

For the preparation of polysulfone films silicon wafers were firstly etched at approximately 40 °C with freshly prepared 3/1 (v/v) sulfuric acid/hydrogen peroxide solution, then rinsed with Milli-Q water and finally dried under nitrogen. These wafers were spin coated (SCI-30 spin coater, LOT Oriel) with a 100 g/L solution of PSf in dichlorobenzene for 30 s at 3600 rpm and then dried over night at 60 °C.

Polymer solutions for the surface functionalizations were prepared by dissolving the polymers in DMAc as first step and then adding Milli-Q water resulting in a 25% (v/v) solution of DMAc. The resulting error of volume contraction was neglected. This procedure was chosen as the polymers were not soluble when directly adding 25% (v/v) DMAc. The PSf-coated wafers were placed in polymer solutions of different concentrations, tightly covered and kept at room temperature for 18 h. Thereafter, the films were gently rinsed with Milli-Q water, dried firstly with nitrogen and subsequently in an oven at 60 °C.

For long term stability tests these modified substrates were stored in Milli-Q water at room temperature for 4 days. They were rinsed once again with Milli-Q water, dried with nitrogen and finally in an oven at 60 °C for 1 h.

2.3. Measurements

2.3.1. Polymer characterization

Size exclusion chromatography (SEC) was performed in DMF containing 0.01 mol/L LiBr at 23 °C with a HPLC system based on a Waters 590 pump, a Shodex RI-71 detector and MZ SDplus columns effective in the 50–5000, 1000–70 000 and 100–2 000 000 molecular weight ranges (all numbers in g/mol). For calibration poly(methyl methacrylate) (PMMA) standards were used.

^{1}H-NMR spectra were recorded in $CDCl_3$ with a Bruker DMX-300 (300 MHz) or Bruker DMX-500 (500 MHz) at 25 °C.

Determination of the BA conversion during ATRP was performed by injecting diluted samples in THF at a temperature of 250 °C on a Shimadzu GC-2010. A methyl silicone fluid column (length: 12 m, 0.2 mm i.d., film thickness 0.2 μm) was employed as stationary phase and hydrogen gas as mobile phase. The following temperature program was conducted: 30 s at 80 °C, heating at 40 °C/min up to 180 °C. The components were detected by a flame ionization detector operating at 250 °C. Each sample was measured at least three times.

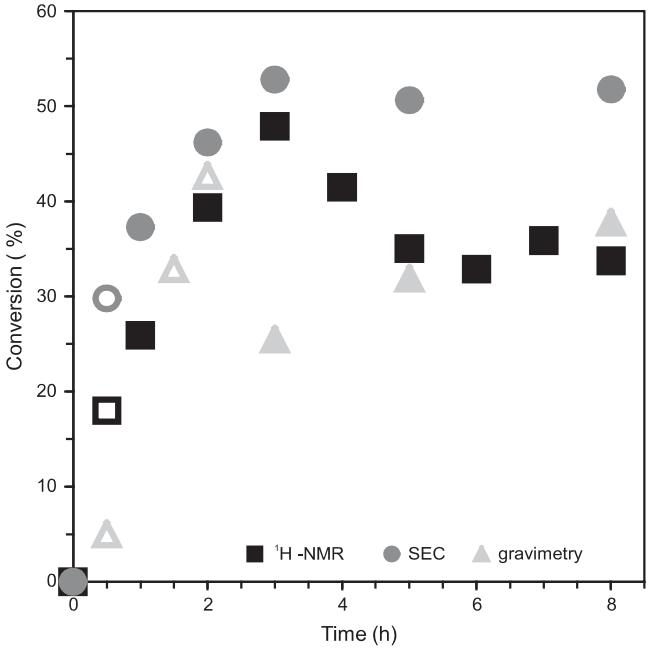

Fig. 2. Comparison of conversion dependence on time for ATRP of NIPAAm ([NIPAAm]:[ECIP]:[CuCl]:[Me_6TREN] 500:1:2:2), determined via ^{1}H-NMR, SEC and gravimetry; open symbols represent experiments in large scale; errors of each method are discussed in the text.

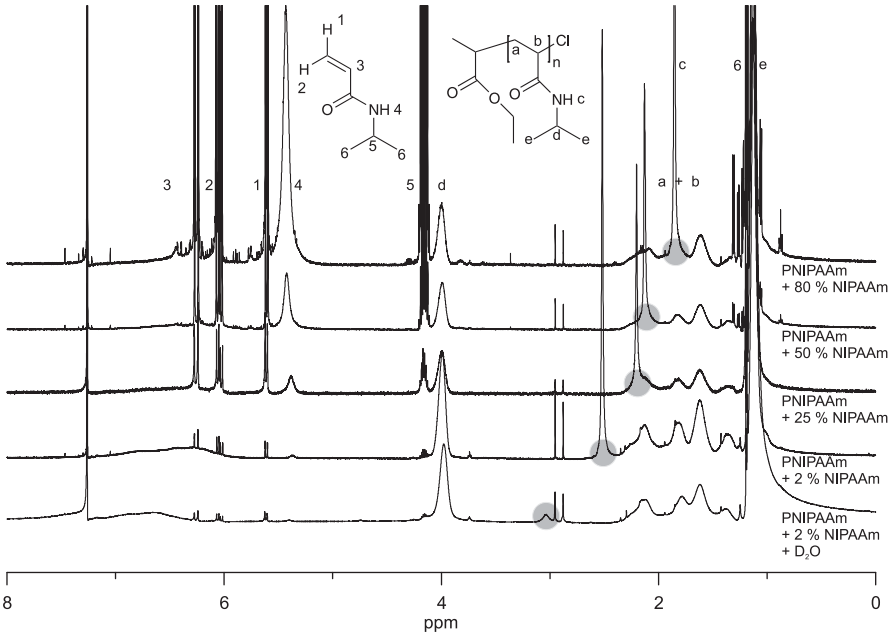

Fig. 3. ^{1}H-NMR spectra (500 MHz) for PNIPAAm in $CDCl_3$ after proton exchange of the N–H group of the polymer (signal highlighted in grey) by addition of water (first spectra) and by addition of monomer in different concentrations.

The critical micelle concentration (CMC) of the block copolymers was determined based on changes in the ratio of the two fluorescence maxima of pyrene upon micelle formation [28] by using a Varian Cary Eclipse fluorescence spectrometer.

For the determination of the block copolymer's LCST, dynamic light scattering (DLS) was performed using a Zetasizer 3000 Hs from Malvern Instruments. The block copolymer was dissolved in DMAc (1% (w/w)), and this solution was dialyzed against Milli-Q water for 4 days using a ZelluTransV regenerated cellulose membrane (MWCO: 1000 g/mol, Carl Roth). The obtained opaque solution was filtered with a 0.2 μm cellulose acetate membrane syringe filter (Nalgene) prior to the DLS measurements. The temperature dependent measurements were performed in intervals of 1 °C equilibrating the system for 5 min at each temperature.

2.3.2. Contact angle measurements

Contact angles (CA) were determined using an optical measurement system (OCA 15 Plus, Dataphysics GmbH, Filderstadt, Germany). Static CAs were measured using the captive bubble method: an air bubble of 5 μL is injected from a 0.5 mL Hamilton syringe with a bent stainless steel needle with an inner diameter of 0.26 mm onto the inverted sample surface immersed into Milli-Q water. All samples were equilibrated for at least 1 min in Milli-Q water before measurement. For temperature dependent static contact angles the temperature of the Milli-Q water was raised to 40 ± 1.1 °C.

Dynamic CAs were measured with the sessile drop method for technical reasons. Using the same syringe but with a straight needle a drop of Milli-Q water was placed onto the surface. With the needle remaining inside the drop advancing (CA_{adv}) and receding (CA_{rec}) contact angles were measured by increasing and decreasing the water volume of the drop with a rate of 0.5 μL/s, respectively.

For both methods the Dataphysics software was used for estimation of the contact angle values. For each value at least three drops or bubbles were measured for one sample and data for each surface were averaged over values for three independently prepared samples. The data presented is given as a mean value and standard deviation. The hysteresis is calculated from the advancing and receding values as follows:

$$\Delta CA = CA_{adv} - CA_{rec} \quad (2)$$

3. Results and discussion

3.1. Polymerization of NIPAAm

Despite the rapid growth in number of publications devoted to the synthesis and the properties of poly(*N*-isopropylacrylamide) the polymerization of NIPAAm using ATRP still remains challenging and is discussed in literature. Nearly at the same time the groups of Matyjaszewski [29] and Brittain [30] reported that ATRP of *N*,*N*-dimethylacrylamide and also of other acrylamides suffered from: 1. inactivation of the catalyst by complexation of copper by the forming polymer, 2. low values of the ATRP equilibrium constant due to a strong bond between the terminal (meth)-acrylamide unit in the polymer and the terminating halide atom and 3. nucleophilic displacement of the terminal halide atom by the amide group. Nevertheless, Masci et al. firstly reported well controlled ATRP of NIPAAm with linear first order kinetic plots as well as controlled molecular weights and low PDIs [31]. The chosen solvents for the polymerization were mixtures of DMF and water as DMF is able to solubilize a wide range of hydrophilic and hydrophobic polymers. Therefore several monomers could in principle be block copolymerized with NIPAAm by adjusting the DMF/water ratio. The influence of the solvent system on polymerization was further used and investigated [32], including work with pure DMF [33]. Taking into account all different aspects of these investigations in this work a pure DMF solvent system was chosen to guarantee the solubility of both monomers NIPAAm and BA and furthermore of their corresponding polymers so that they could be used as macroinitiators to result in block copolymers. Additionally, a beneficial effect of a solvent being capable to form hydrogen-bonding to monomer and polymer was anticipated,

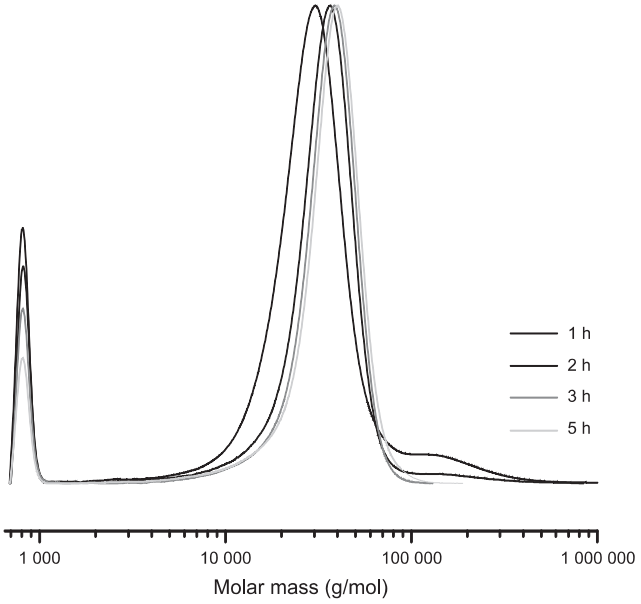

Fig. 4. Comparison of monomer and polymer signals in SEC traces with increasing polymerization time for ATRP of NIPAAm ([NIPAAm]:[EClP]:[CuCl]:[Me_6TREN] 500:1:2:2).

because it reduces the known deactivation of the catalyst by acrylamides and their polymers [34]. Furthermore chloride and no bromide systems were used in order to reduce the probability of substitution reactions.

Considering the controversial discussion of the degree of livingness and control of the polymerization of NIPAAm in literature time resolved ATRP was performed in the initial stage of this work. Thereby, first order kinetic plots and an increase of resulting molar mass with increasing conversion could be obtained. Conversion was obtained using three different techniques. Fig. 2 compares the values obtained via integration of the monomer and polymer peaks either by ^{1}H-NMR spectroscopy or by SEC for a time resolved polymerization of NIPAAm (conditions see below) and the gravimetrically obtained yield. The resulting conversions by NMR spectroscopy and SEC differ by at least 10% due to different errors related to each method.

Using ^{1}H-NMR decreasing values of the conversion at higher polymerization times were observed. In order to explain this unexpected result, some more NMR experiments using PNIPAAm and added monomer were performed. Interestingly, a shift of the N–H peak of the polymer was observed while adding more monomer, but no other chemical shift change could be observed as can seen in Fig. 3.

When D_2O is added to the polymer solution the N–H peak is shifted downfield and intensity decreases due to hydrogen exchange. When monomer is added this peak can be observed with a shift to the upfield region and intensity does not change. This indicates that the proton exchange which takes place is different for water and monomer polymer solutions. Although the exchange process was not investigated further these observations are strong indications for an aggregation taking place between the monomer and the polymer. As formation of aggregates depends on the concentration of the monomer (cf. Fig. 3) and because this is changing during polymerization, the method of determining conversions via ^{1}H-NMR spectroscopy has a systematic error.

Conversions obtained by SEC also resulted in reasonable values. It is considered that the determined area of the monomer peak is normally estimated too small as can be seen in Fig. 4. As a consequence the conversions are always too high and this is confirmed by comparison to those obtained by NMR spectroscopy (cf. Fig. 2). Nevertheless, the same curvature of the curve for time-dependent conversion could be observed leading to the same information regarding control and livingness of the polymerization.

Additionally, gravimetric polymer yield was calculated for selected samples. As the amounts precipitated from relatively small samples (1 mL) were small the error resulting from this method is quite high. In addition with increasing conversion the solutions get more viscous and, consequently, the error changes with polymerization time. Nevertheless, for a sample which was polymerized to 35.1% conversion according to ^{1}H-NMR spectroscopy and 50.7% according to SEC, a yield of 31.9% was observed according to gravimetry which, considering the individual errors, correlates well. However, overall relative deviations by up to 50% for gravimetric yields were observed.

In summary the determination of conversion using these three different methods comprises individual errors related to each technique. In the following the presented conversions rely on the integration of monomer and polymer peak by ^{1}H-NMR spectroscopy because the resulting error due to polymer/monomer aggregation is judged to be the smallest and will therefore be neglected.

Polymerization of NIPAAm was conducted using different ratios of monomer to initiator by keeping the monomer concentration constant. The resulting first order kinetic plots show a nearly linear relationship for 3 h reaction time when considering the persistent radical effect (PRE) [35,36] (Fig. 5).

As expected the conversion decreases with increasing monomer to initiator ratio due to the decreasing rate of reaction with decreasing initiator concentration. After 3 h all conversions level off and plateau values are reached. The end of chain extension after this time could also be proven by determination of the molar masses which do not increase any longer for all reaction conditions. However, during the 3 h of reaction a linear relationship for the increase of molar masses

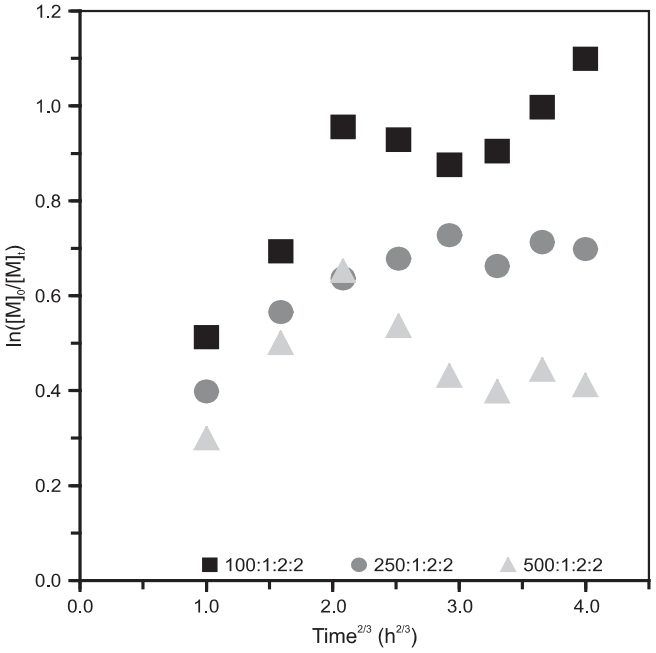

Fig. 5. Time dependency of $\ln([M]_0/[M]_t)$ according to the persistent radical effect for ATRP of NIPAAm with changing monomer ratios [NIPAAm]:[EClP]:[CuCl]:[Me_6TREN] given in the diagram; $[NIPAAm]_0 = 3.9$ mol/L in DMF at room temperature; $[NIPAAm]_0/[NIPAAm]_t$ determined via ^{1}H-NMR spectroscopy.

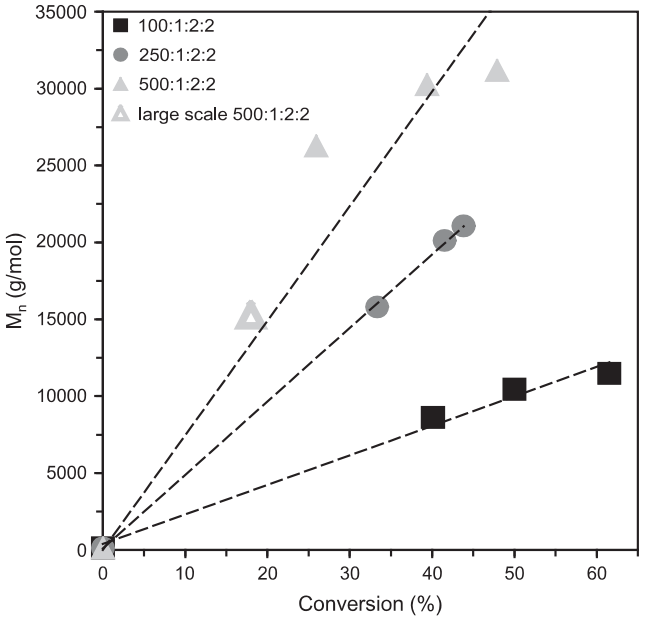

Fig. 6. Molar mass dependency of conversion determined via ^{1}H-NMR for ATRP of NIPAAm with changing monomer ratios [NIPAAm]:[EClP]:[CuCl]:[Me_6TREN] given in the diagram; $[NIPAAm]_0 = 3.9$ mol/L in DMF at room temperature.

can be observed with the exception of the polymerization using a 500:1 monomer to initiator ratio (Fig. 6). It should be noted that the SEC trace of this polymerization mixture also shows a shoulder at higher molar masses indicating that termination by recombination takes place in the very beginning of the reaction (cf. Fig. 4). Nevertheless, the resulting PDIs are ~1.2 for all polymerizations.

The observed level off of the polymerization of NIPAAm can be related to the discussion of its living character in literature. Such level off for *N*,*N*-dimethylacrylamide in DMF has been already observed [37]. On the one hand this is a clear indication of termination reactions which should be suppressed in a living polymerization. But actually this cannot be the only reason for the decay of reaction rate because the PDIs remain low (~1.2). On the other hand there is a linear first order kinetic plot for up to 3 h. These are typical characteristics for a well controlled living polymerization mechanism. The whole polymerization process is even more complicated as the used complex with Me_6TREN as ligand is known to disproportionate in DMF and thereby Cu(0) is formed [38,39]. This could be proven by the observation of a reddish brown precipitate during polymerization. The formed Cu(0) surely has an influence on the control and mechanism of the polymerization. Another interesting point is the fact that all polymerizations seem to stop after approximately 3 h. In this context catalyst deactivation cannot be the dominating contribution as catalyst concentration decreases with increasing monomer to initiator ratio. Hence, polymerizations with lower catalyst concentration should stop earlier than those for mixtures containing more copper complex.

In conclusion, similar to literature, ambiguous results with respect to the livingness of the polymerization of NIPAAm were obtained. Further investigations were made by testing whether the obtained polymers were able to act as macroinitiator and thereby add a second block of PBA. Indeed, by polymerizing NIPAAm via ATRP with DMF as solvent, Me_6TREN as ligand and a chloride system control over molecular weight and a low PDI were gained and finally very reproducible results were obtained; this was confirmed by identical results for the preparations performed in large scale as compared to data from the kinetics experiments (cf. Fig. 2).

3.2. Polymerization of BA

ATRP of BA has been widely investigated, but mainly using bulk or near bulk systems [40,41]. Bulk polymerization bears the problem of poor solubility of the deactivator and results in a poor control of the polymerization. The addition of even small amounts of a good solvent for the Cu(II) complex such as DMF improves reaction conditions with regard to control [41,42]. For this work bulk polymerization could not be applied, because for the preparation of block copolymers the macroinitiator has to be soluble in the reaction medium. As the solubility of PNIPAAm as macroinitiator in BA is poor and in order to keep reaction conditions as simple as possible the same reaction conditions as for the polymerization of NIPAAm were applied to BA, too. The very reactive ligand Me_6TREN has been already applied for the polymerization of BA [43,44] and also in increased ratios of ligand to initiator (2:1) [45]. However, in the chosen system of ligand and solvent disproportion of Cu(I) is pronounced as mentioned before.

Polymerization of BA was conducted in a time resolved manner determining the conversion via GC. As can be seen in Fig. 7 the analysis of the first order kinetic plot according to the PRE is difficult due to the high error.

This error is based on the evaporation of the monomer during the polymerization process as it was conducted at 70 °C and under a slight pressure of argon. Taking the error bars into account, kinetic curves for all polymerizations are not linear and hence terminations take place. Molar masses do not increase after 2 h any longer. Additionally PDIs with values around 1.5 (see Table 1) were determined supporting the assumption of termination reactions. However, polymerization took place using these conditions and therefore these polymers were tested whether they are able to reinitiate.

In parallel, the reaction conditions were changed: the less reactive ligand *N*,*N*,*N*′,*N*′,*N*″-pentamethyldiethylenetriamine and the initiator ethyl α-bromoisobutyrate (EBriB) were used. In parallel the temperature was reduced to 50 °C and the monomer concentration was increased. These changes resulted in linear first order kinetic plots, a linearly evolving molar mass with conversion and

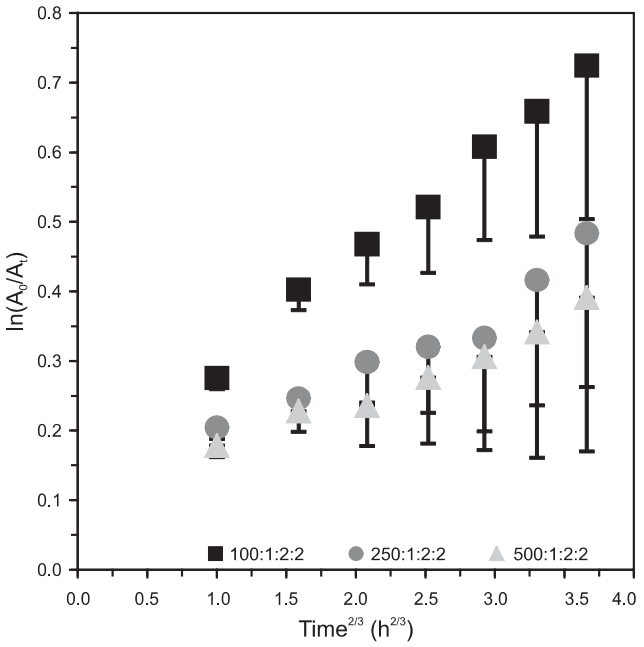

Fig. 7. Time dependency of $\ln(A_0/A_t)$ according to the persistent radical effect for ATRP of BA with changing monomer ratios [BA]:[EClP]:[CuCl]:[Me_6TREN] given in the diagram; $[BA]_0 = 3.58$ mol/L in DMF at 70 °C; A_0/A_t determined via GC using dodecane as internal standard; error due to evaporation of monomer during polymerization.

Table 1
Conditions for synthesis of the block copolymers and results of characterization by SEC.

1. Block	[M]:[ini]: [CuCl]:[L]	Time (min)	M_n (g/mol)	M_w/M_n		2. Block	[M]:[macroini]: [CuCl]:[L]	Time (min)	M_n (g/mol)	M_w/M_n	
PNIPAAm	500:1:2:2	180	33 500	1.13		PBA	500:1:2:2	0–420	No reinitiation		
PNIPAAm	500:1:2:2	90	29 400	1.16		PBA	500:1:2:2	0–420	No reinitiation		
PNIPAAm	500:1:2:2	30	15 300	1.15		PBA	500:1:2:2	0–420	No reinitiation		
PNIPAAm	500:1:2:2	120	32 900	1.15	#1						
PBA	500:1:2:2	90	19 900	1.67		PNIPAAm	500:1:2:2	420	58 300	1.20	#2
PBA	250:1:2:2	90	7500	1.62		PNIPAAm	250:1:2:2	120	37 500	1.18	#3
PBA	250:1:2:2	150	15 000	1.56		PNIPAAm	250:1:2:2	120	37 800	1.22	#4
PBA	100:1:2:2	30	3900	1.14		PNIPAAm	100:1:2:2	180	25 000	1.13	#5

PDIs around 1.1 (Fig. 8). Additionally the systematic error due to evaporation of the monomer could be reduced drastically.

3.3. Preparation of block copolymers

Syntheses of block copolymers were attempted using two approaches: either taking PNIPAAm as macroinitiator and add a PBA block or vice versa. PNIPAAm macroinitiators of different molecular weights were synthesized by a step-wise variation of the polymerization time. All polymers show PDIs < 1.2 (cf. Table 1). Attempts toward block copolymerization were conducted in a time resolved manner by taking samples every hour. However, for all PNIPAAm samples no reinitiation could be observed after up to 7 h. Neither by SEC an increase of molecular weight could be revealed, nor characteristic bands for PBA were found by ^{1}H-NMR spectroscopy or IR spectroscopy. This means that although linear first order kinetic plots, linear molar mass to conversion plots and low PDIs were found during synthesis (cf. above), the polymerization of NIPAAm lacks one characteristic of livingness: the resulting polymers could not be reinitiated by BA. This fact supports the assumption that loss of end groups takes place, but still PDIs are very low. It has been demonstrated that surface initiated ATRP of PNIPAAm in track etched membranes using the same reaction conditions as described here was well controlled [46]. In that study, the reinitiation of grafted PNIPAAm chains by NIPAAm and also by *tert*-BA has been shown. Considering the results of the work presented here, livingness of ATRP of NIPAAm in the used reaction conditions still remains an issue to be investigated further.

Next, PBA samples of different molecular weights were used as macroinitiators and reinitiated with NIPAAm. Although the polymerization of BA had been poorly controlled chain extension with PNIPAAm could be observed by SEC (cf. Table 1), ^{1}H-NMR and IR spectroscopy. Additionally one reinitiation experiment was followed in a time resolved manner and the same dependency between $\ln(A_0/A_t)$ and $t^{2/3}$ was observed as for polymerization of NIPAAm without macroinitiator (cf. Fig. 5). Even a level off at similar polymerization time was observed (Fig. 9).

Another proof for the relatively poor livingness of the polymerization of BA (to prepare the macroinitiator for NIPAAm) can be seen when looking at the SEC traces (Fig. 10).

Depending on polymerization time a shoulder of increasing intensity can be seen appearing at the initial molar mass of the macroinitiator. Nevertheless the main peak is shifted to higher molar masses. In order to obtain pure block copolymer without fractions of homo PBA (due to "dead" chain ends which are not able to function as macroinitiator) the mixture was precipitated once again. For that purpose heptane (Hildebrand parameter 15.1 MPa$^{1/2}$ [47]) was chosen as it is able to dissolve PBA (20.4 MPa$^{1/2}$ [48]) more easily than PNIPAAm (22.9 MPa$^{1/2}$ [49]), and thereby selective dissolution of the block copolymer should be achieved. This purification was successful as could be proven by SEC (cf. Fig. 10), and finally apparent PDIs $\sim$ 1.2 were obtained which agree with the values obtained for the polymerization of NIPAAm with the low-molar mass initiator (cf. above).

3.4. Characterization of block copolymers

The resulting block copolymers (#3–#5; cf. Table 1) were characterized with respect to real molar mass, LCST and critical micelle concentration (CMC). As the molecular weights were determined via SEC calibrated with PMMA the results include an error. The chemical composition and thereby solubility of PMMA resembles more PBA than PNIPAAm. This means that the error is higher for the PNIPAAm-containing polymers. This error is not estimated to depend linearly on molecular weight, and additionally the influence of the second block is unknown. Therefore, molecular weights were recalculated using ^{1}H-NMR intensities for the respective blocks in order to estimate the block ratio and the molecular weights of the PBA macroinitiator. These results for the block copolymers with three different molecular weights and different ratios of PBA to PNIPAAm are summarized in Table 2.

Solubility of block copolymer #3 in water was very poor, therefore solutions to determine the LCST were prepared by dissolving the polymer in DMAc in the first step and then dialyzing this solution against water. This procedure worked also for block copolymer #5, but in polymer #4 the PBA block is apparently too long so that no aqueous solution could be prepared. The resulting aqueous solutions of block copolymers #3 and #5 were slightly opaque. Both LCSTs were determined to be 32 °C. For polymer #3 with a high molecular weight the precipitation at the LCST was irreversible; the block copolymer did not dissolve again after cooling down the sample. In contrast, polymer #5 did dissolve again; it was proven that the transition was reversible. After first determination of the LCST a small amount of precipitate was left at the bottom of the cell which dissolved after cooling. Due to the low molecular weight of the block copolymer the resulting contribution of the small PBA block to the solubility of the block copolymer in water is low. That is why only the phase transition of polymer #5 is reversible.

Critical micelle concentrations were determined using 25 vol% DMAc solutions which were later used for the surface functionalization. Obviously, polymer #3 with a higher molecular weight compared to polymer #5 showed a lower CMC: 2.8 μmol/L in comparison to 9.6 μmol/L, respectively. These values correspond to concentrations of $\sim$0.1 g/L. This demonstrates that solubility of both block copolymers is significantly increased by the addition of DMAc to water (CMC of polymer #3 in water $<$0.001 g/L).

3.5. Preparation and characterization of temperature-switchable surfaces

Because of the low solubility of the block copolymers in water on the one hand and the need of aqueous solution for surface modification of polysulfone via adsorption from an aqueous solution on the other hand, a solvent mixture was chosen to enhance

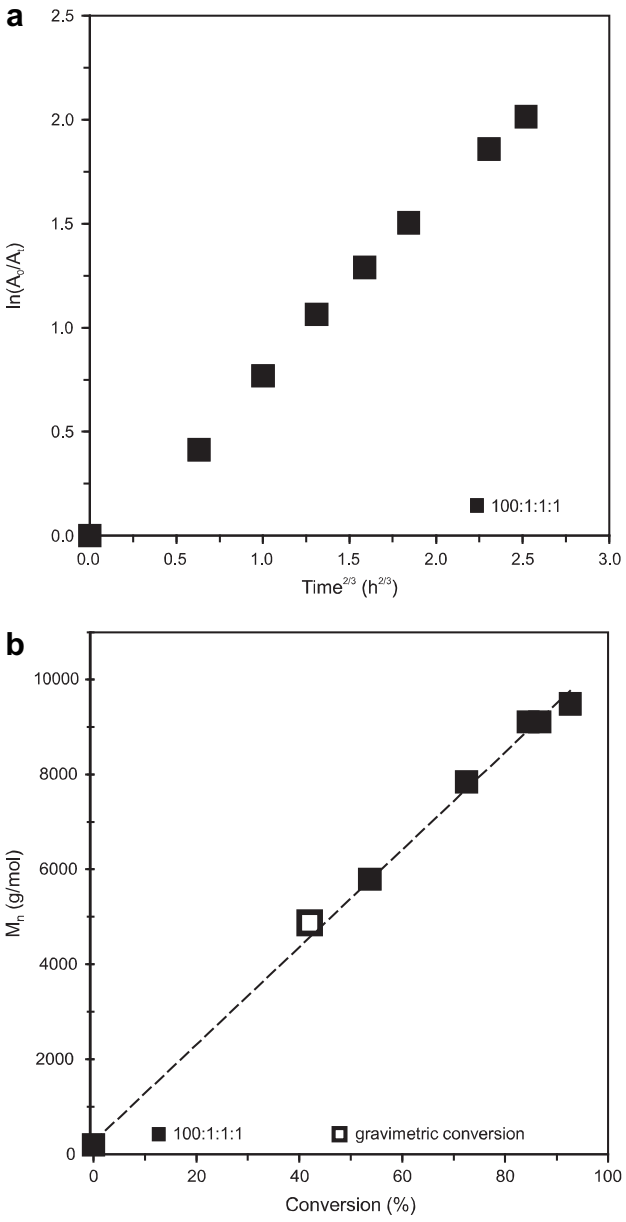

Fig. 8. ATRP of BA with [BA]:[EBriB]:[CuBr]:[PMDETA] 100:1:1:1, $[BA]_0 = 7$ mol/L in DMF at 50 °C; (a) time dependency of $\ln(A_0/A_t)$ according to the persistent radical effect; A_0/A_t determined via GC using dodecane as internal standard (y axis error bars ≤ 0.03); (b) molar mass dependency of conversion determined via GC; open symbol represents experiment in large scale, here conversion was determined gravimetrically.

solubility of the polymers. Additionally, this solvent should also swell the PSf film onto which the block copolymers should be adsorbed. Because of their chemical similarity the PBA block can penetrate the PSf surface layer which collapses again after exposure of the sample to pure water. This anticipated physical network (obtained by "surface entrapment") should result in a firm anchoring of the block copolymer in the PSf surface layer and therefore enhance the long term stability of such a surface functionalization. Such "surface entrapment" had first been proposed by Ruckenstein and Chung [50]. DMAc was chosen as cosolvent as it is miscible with water and dissolves the block copolymer better than the PSf layer.

For the surface functionalization the block copolymers #3 and #5 and homo polymer #1 (as a reference material with similar molar mass as #3, but lacking the ability to be anchored via "surface entrapment") were dissolved in 25 vol% aqueous DMAc. The substrates with spin coated PSf films were incubated in polymer solutions of different concentrations. Pure PBA was not tested as a reference material, because results are not anticipated to give much information.

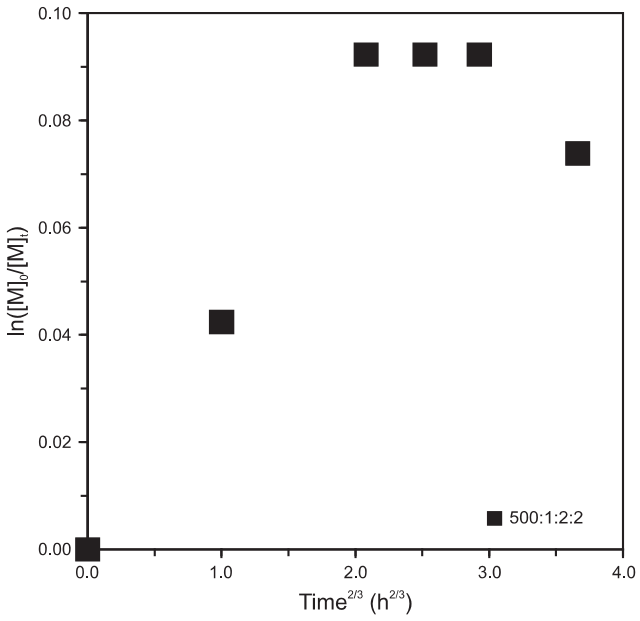

Fig. 9. Time dependency of $\ln([M]_0/[M]_t)$ according to the persistent radical effect for ATRP of NIPAAm with [NIPAAm]:[PBA-Cl]:[CuCl]:[Me_6TREN] 500:1:2:2; $[NIPAAm]_0 = 3.9$ mol/L in DMF at room temperature; $[NIPAAm]_0/[NIPAAm]_t$ determined via ^{1}H-NMR spectroscopy.

Functionalization of the PSf films was characterized by measurement of contact angle. Directly after modification all materials reveal a much lower contact angle than for PSf indicating significant surface hydrophilization (Table 3).

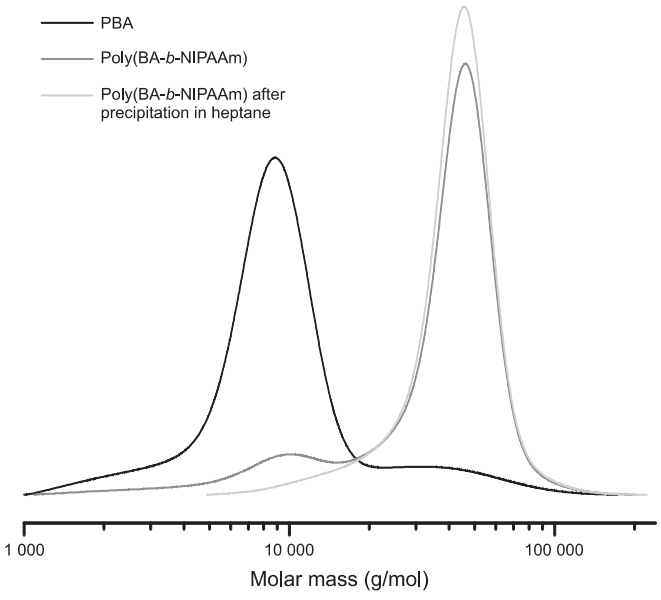

Fig. 10. SEC traces for chain extension of PBA ([BA]:[EClP]:[CuCl]:[Me_6TREN] 250:1:2:2, $c(BA) = 3.58$ mol/L, 70 °C in DMF) by NIPAAm ([NIPAAm]:[PBA-Cl]:[CuCl]:[Me_6TREN] 250:1:2:2, $c(NIPAAm) = 3.9$ mol/L, 25 °C in DMF) via ATRP and subsequent purification of the resulting block copolymer by precipitation in n-heptane.

Table 2
Characterization of block copolymers concerning composition, estimated molecular weight, critical micelle concentration and lower critical solution temperature.

	% NIPAAm via ^{1}H-NMR	M_n calculated via ^{1}H-NMR (g/mol)	CMC (g/L, μmol/L) in 25% aqueous DMAc	LCST via DLS (°C)
#1	Homopolymer			
#3	62	39 500	0.11, 2.8	32, irreversible
#4	29	25 900	Not detectable	
#5	51	8000	0.08, 9.6	32, reversible

For the homo polymer #1 the expected trend can be observed in Fig. 11. With decreasing polymer concentration the resulting contact angle increases, i.e. less PNIPAAm has been adsorbed to the PSf surface. For concentrations of 0.01 g/L and 0.001 g/L no differences in contact angle can be observed. Looking at both block copolymers another relationship is observed. With decreasing polymer concentration (from 1 g/L to 0.01 g/L) the contact angles decrease, too. Samples prepared with a concentration of 0.01 g/L block copolymer exhibit the most hydrophilic character. This trend is even more pronounced for block copolymer #5 with a lower molecular weight compared to copolymer #3. However, in both cases block copolymer concentrations of 0.001 g/L resulted in surfaces with higher contact angles than the minimum values. Overall, the small degrees of modification are not related to a pronounced decrease of polymer concentration in the solution while it accumulates at the surface.

These different trends for the block copolymers compared to the homo polymer can be taken as evidence for a contribution of amphiphilic properties of the block copolymers and their ability to form micelles to the efficiency of surface functionalization. Both block copolymers show CMCs around 0.1 g/L. The big difference in contact angles achieved by solutions with micelles (1–0.1 g/L) and without micelles (0.01–0.001 g/L) could be due to micelle adsorption in the first case. In the washing step, adsorbed micelles might be removed much easier than adsorbed macromolecules. The fact that the best modification efficiency for the PSf films is obtained for block copolymer concentrations of 0.01 g/L verifies that selective adsorption of the hydrophobic PBA block in the macromolecules is successful. In addition an even more pronounced modification is obtained for block copolymer #5. The molar mass of this polymer is quite low and it contains a shorter PBA block in comparison to block copolymer #3. This could lead to less efficient entrapping.

Table 3
Long term stability of surface functionalization determined via measurement of contact angles using the captive bubble method directly after modification (start) and after 4 days in water as well as contact angle hysteresis after 4 days in water from measurement of contact angles using the sessile drop method.

	[Polymer] (g/L)	Contact angle at start (°)	Contact angle after 4 days (°)	CA hysteresis after 4 days (°)
Bare PSf	0	80.1±0.8	71.8±1.5	24.9±1.5
Homo polymer #1	0.001	61.0±5.3	73.1±0.5	23.6±2.5
	0.01	60.4±2.5	66.7±5.5	26.5±1.2
	0.1	49.6±2.4	57.5±9.6	26.9±0.9
	1	49.0±1.0	52.5±2.1	28.4±1.7
Block copolymer #3	0.001	66.6±0.8	64.9±0.0	25.2±2.7
	0.01	52.0±4.3	55.3±1.3	29.1±0.3
	0.1	54.3±2.2	52.2±2.0	20.3±3.4
	1	55.8±2.7	54.2±0.6	20.3±1.8
Block copolymer #5	0.001	75.3±3.9	69.2±4.2	24.9±3.4
	0.01	44.3±1.8	59.4±4.4	21.7±4.2
	0.1	47.7±4.3	56.2±3.0	27.8±0.2
	1	51.2±4.7	54.7±1.1	22.8±1.4

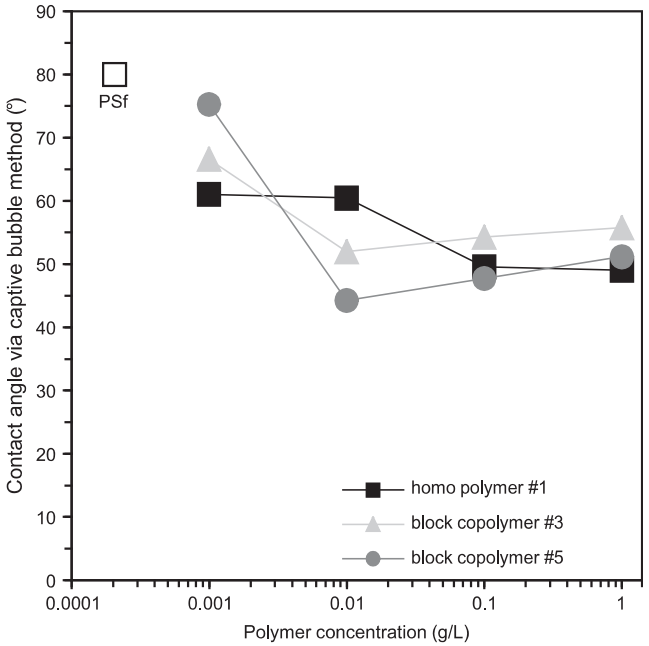

Fig. 11. Dependency of the average contact angle of the modified PSf films with homo polymer #1 and block copolymers #3 and #5 prepared from solutions with different polymer concentrations in comparison to bare PSf, standard deviations are given in Table 3.

That hypothesis can also be proven by long term stability tests. The functionalized materials were stored in an excess of water for four days in order to reach the desorption equilibrium. In case of leaching of adsorbed/entrapped PNIPAAm-containing polymer the films should get more hydrophobic. Table 3 shows that contact angles for all samples prepared with homo polymer #1 consistently increase irrespective of the polymer concentration used for modification. Nevertheless, the resulting contact angles remained below the value for pure PSf indicating that a fraction of this adsorptive modification is stable. As the contact angle remains nearly constant for samples prepared with block copolymer #3 this functionalization is stable. This result in principle proves the hypothesis that an anchor block linked to the active component PNIPAAm enhances long term stability of a surface functionalization. But this statement cannot be generalized. Block copolymer #5 does leach out to some extent as the observed contact angles at equilibrium increase relative to the state directly after modification. Hence, a sufficient length of the anchor block (such as in block copolymer #3) is needed to result in stable surface functionalization via adsorption/"surface entrapping".

The observations with respect to leaching out can be underlined taking also the results of dynamic contact angle measurements into account (cf. Table 3). The CA hysteresis for pure PSf films after four days storage in water is $24.9 \pm 1.5°$. This value is reached or even exceeded for samples prepared using homo polymer #1. As a small fraction of the modification is stable (cf. above), this leads to a higher inhomogeneity of the polymer surface than for pure PSf resulting in a higher value for the hysteresis. Preparations using block copolymer #5 show, considering the experimental error, almost constant CA hysteresis. Block copolymer #3 which resulted in stable functionalization (captive bubble contact angles remained constant over time) leads to lower CA hysteresis than PSf for polymer concentrations of 1 g/L and 0.1 g/L. This is a further indication that modification was successful and leads to a relatively high surface coverage of PSf with grafted PNIPAAm. For block copolymer concentrations of 0.01 g/L and 0.001 g/L CA hysteresis

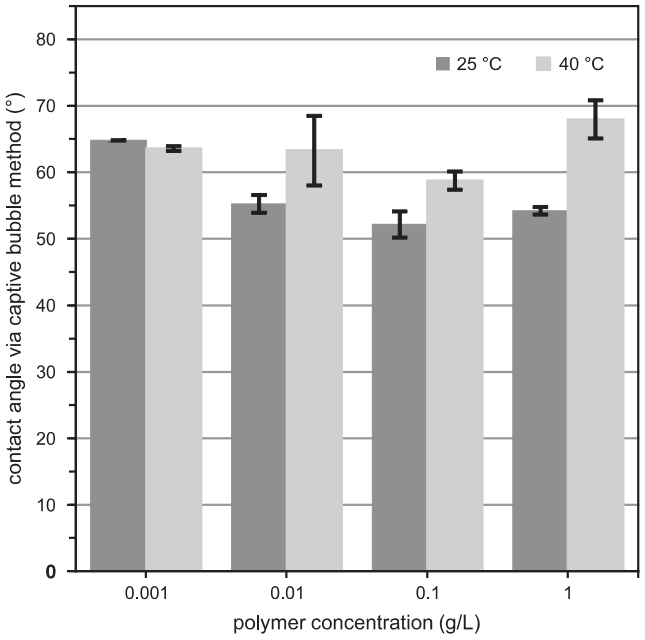

Fig. 12. Contact angle at temperatures around the LCST of PNIPAAm of surfaces functionalized with block copolymer #3 measured via captive bubble method.

resembles that for PSf or is even higher; this trend is in line with a decreasing surface coverage of PSf by grafted PNIPAAm.

Finally, the stable PNIPAAm-grafted PSf films were characterized concerning their switching effect at different temperatures. For the realization of a "chaotic surface" as outlined in the Introduction its properties with respect to wettability have to change reversibly at temperatures near the LCST of PNIPAAm. This property was tested by heating the surrounding solution not the surface itself. Comparison of contact angles at 20 °C and 40 °C shows that films prepared via functionalization with block copolymer #3 concentrations of 1–0.01 g/L become considerably more hydrophobic at temperatures above the LCST (Fig. 12). A comparison between the obtained contact angle values and those published is inconclusive because the data in the literature is already inconsistent [51].

In contrast to the switchability of block copolymer #3 in solution (irreversibly precipitation was observed; cf. above) the switching effect is reversible for the surface-anchored PNIPAAm. As the samples prepared from a 0.001 g/L block copolymer solution showed a lower degree of modification (surface coverage; as indicated by their higher contact angle) it is not surprising that a switching effect could not be detected in this case. However, the most important result of this part of the study is that by optimization of block copolymer composition and using high enough concentration in an aqueous solution of suited composition during the adsorption/"entrapping" step, a stable and temperature-switchable surface functionalization was obtained.

4. Conclusions

Surfaces exhibiting switchable properties with respect to wettability depending on the external stimulus temperature have been prepared. In order to achieve that goal, the synthesis of well defined block copolymers containing PNIPAAm and PBA has been investigated. The polymerization of NIPAAm using ATRP was controlled with respect to obtained molecular weight in the range of 10–30 kDa and PDIs < 1.2, but, as PNIPAAm could not be reinitiated when used as macroinitiator, the polymerization followed no living mechanism as already discussed in literature. As a consequence block copolymers were only accessible using PBA as macroinitiator. Because limited livingness of ATRP of BA was observed using Me_6TREN as ligand and a CuCl system in DMF, the polymerization conditions were changed using PMDETA as ligand and a CuBr system in DMF as solvent to result in a controlled polymerization of BA. Therefore, for future experiments block copolymers with low PDI should be accessible without the need for a purification step to remove "dead" macroinitiator. The synthesized block copolymers showed different properties in solution due to their chemical composition regarding molecular weight and ratio of PNIPAAm/PBA block length.

Surface functionalization was obtained via adsorbing block copolymers of different composition to a spin coated PSf film. It has been shown that the ability of a poly(BA-*b*-NIPAAm) to anchor in the PSf film depends on the molecular weight of the PBA block. Using a block copolymer with a PBA block of 7500 g/mol "surface entrapment" resulted in a stable surface functionalization which showed no leaching out in water while a homo PNIPAAm desorbed under the same conditions. It should be noted that this method is similar to previous work where the surface modification of PSf or polystyrene via adsorption of amphiphilic poly(ethylene glycol) derivatives from aqueous solutions had been facilitated via interfacial mixing caused by slight swelling of the substrate polymer [19,52]. Using the prepared stable PSf film containing poly(BA-*b*-NIPAAm) the switching effect due to LCST behavior of PNIPAAm at 32 °C was determined and shown to be dependent on the degree of surface functionalization based on the used concentration of the polymer solution for preparation. Those surfaces are very promising for the realization of 'chaotic' surfaces as an anti-biofouling strategy. As the entrapment process is an easily applicable method to modify surfaces the functionalization with the synthesized block copolymer can be extended to various polymeric surfaces (e.g. membrane surfaces) to give them stimuli-responsive properties. Additionally those polymer architectures can be used as firmly anchored surface-segregated additives in polymeric blends.

Acknowledgments

The authors thank Karin Klingelhöller, student at Universität Duisburg-Essen (UDE), and Eric Scalva, student at Colorado State University, Ft. Collins, USA, and supported during his stay in Essen via the RISE program of the German Academic Exchange Foundation (DAAD), for their assistance in polymer synthesis, and Dieter Jacobi (Technische Chemie, UDE) for the SEC analysis.

References

[1] Bos R, van der Mei HC, Busscher HJ. FEMS Microbiol Rev 1999;23:179–230.
[2] Donlan RM. Emerg Infect Dis 2002;8(9):881–90.
[3] Wingender J, Neu TR, Flemming HC. Microbial extracellular polymeric substances. Heidelberg, Berlin: Springer Verlag; 1999.
[4] Davey ME, O'Toole GA. Microbiol Mol Biol Rev 2000;64:847–67.
[5] Omae I. Chem Rev 2003;103:3431–48.
[6] Lewis K, Klibanov AM. Trends Biotechnol 2005;23:343–8.
[7] An YH, Friedman RJ. J Biomed Mater Res (Appl Biomater) 1998;43:338–48.
[8] Callow JA, Callow ME, Ista LK, Lopez G, Chaudhury MK. J R Soc Interface 2005;2:319–25.
[9] Sigal GB, Mrksich M, Whitesides GM. J Am Chem Soc 1998;120:3463–73.
[10] Kane RS, Deschatelets P, Whitesides GM. Langmuir 2003;19:2388–91.
[11] Senaratne W, Andruzzi L, Ober CK. Biomacromolecules 2005;6:2427–48.
[12] Gudipati CS, Finley JA, Callow JA, Callow ME, Wooley KL. Langmuir 2005;21:3044–53.
[13] Krishnan S, Ayothi R, Hexemer A, Finley JA, Sohn KE, Perry R, et al. Langmuir 2006;22:5057–86.
[14] Ista LK, Lopez G. J Ind Microbiol Biotechnol 1998;20:121–5.
[15] Okano T, Yamada N, Sakai H, Sakurai Y. J Biomed Mater Res 1993;27:1243–51.
[16] Ito Y, Chen G, Guan Y, Imanishi Y. Langmuir 1997;13:2756–9.
[17] Ista LK, Perez-Luna VH, Lopez GP. Appl Environ Microbiol 1999;65:1603–9.
[18] Ista LK, Mendez S, Perez-Luna VH, Lopez GP. Langmuir 2001;17:2552–5.
[19] Lazos D, Franzka S, Ulbricht M. Langmuir 2005;21:8774–84.

[20] Chung JE, Yokoyama M, Yamato M, Aoyagi T, Sakurai Y, Okano T. J Control Release 1999;62:115–27.
[21] Braunecker WA, Matyjaszewski K. Prog Polym Sci 2007;32:93–146.
[22] Nuopponen M, Ojala J, Tenhu H. Polymer 2004;45:3643–50.
[23] Licea-Claveríe A, Carrión-García SA, Medina-Urquiza MR, Cornejo-Bravo JM, Hawker CJ, Frank CW. PMSE 2006;95:170–1.
[24] Li G, Shi L, An Y, Zhang W, Ma R. Polymer 2006;47:4581–7.
[25] Li G, Song S, Guo L, Ma S. J Polym Sci Part A Polym Chem 2008;46:5028–35.
[26] Queffelec J, Gaynor SG, Matyjaszewski K. Macromolecules 2000;33:8629–39.
[27] Colombani O, Ruppel M, Schubert F, Zettel H, Pergushov DV, Müller AHE. Macromolecules 2007;40:4338–50.
[28] McPherson T, Kidane A, Szleifer I, Park K. Langmuir 1998;14:176–86.
[29] Teodorescu M, Matyjaszewski K. Macromolecules 1999;32:4826–31.
[30] Rademacher JT, Baum M, Pallack ME, Brittain WJ. Macromolecules 2000;33:284–8.
[31] Masci G, Giacomelli L, Crescenzi V. Macromol Rapid Commun 2004;25:559–64.
[32] Ye J, Narain R. J Phys Chem B 2009;113:676–81.
[33] Nagase K, Kobayashi J, Kikuchi A, Akiyama Y, Kanazawa H, Okano T. Langmuir 2007;23:9409–15.
[34] Xia Y, Yin X, Burke NAD, Stöver HDH. Macromolecules 2005;38:5937–43.
[35] Fischer HJ. J Polym Sci Part A Polym Chem 1999;37:1885–901.
[36] Fukuda T, Goto A, Ohno K. Macromol Rapid Commun 2000;21:151–65.
[37] Teodorescu M, Matyjaszewski K. Macromol Rapid Commun 2000;21:190–4.
[38] Matyjaszewski K, Tsarevsky NV, Braunecker WA, Dong H, Huang J, Jakubowski W, et al. Macromolecules 2007;40:7795–806.
[39] Percec V, Guliashvili T, Ladislaw JS, Wistrand A, Stjerndahl A, Sienkowska MJ, et al. J Am Chem Soc 2006;128:14156–65.
[40] Davis KA, Matyjaszewski K. Macromolecules 2000;33:4039–47.
[41] Huang J, Pintauer T, Matyjaszewski K. J Polym Sci Part A Polym Chem 2004;42:3285–92.
[42] Reyes M, Yu X, Shipp DA. Macromol Chem Phys 2001;202:3268–72.
[43] Xia J, Gaynor SG, Matyjaszewski K. Macromolecules 1998;31:5958–9.
[44] Inoue Y, Matyjaszewski K. Macromolecules 2004;37:4014–21.
[45] Ohno S, Matyjaszewski K. J Polym Sci Part A Polym Chem 2006;44:5454–67.
[46] Friebe A, Ulbricht M. Macromolecules 2009;42:1838–48.
[47] Brandrup J, Immergut EH, Grulke EA. Polymer handbook. New York: Wiley Interscience Publication; 1999.
[48] Barton AFM. CRC handbook of polymer–liquid interaction parameters and solubility parameters. New York: CRC Press; 1990.
[49] Ahmad HJ. Macromol Sci Chem A 1982;17(4):585–600.
[50] Ruckenstein E, Chung DB. J Colloid Interface Sci 1988;123:170–85.
[51] Gilcreest VP, Carroll WM, Rochev YA, Blute I, Dawson KA, Gorelov AV. Langmuir 2004;20:10138–45.
[52] Tarnawski R, Ulbricht M. Colloids and Surfaces A, submitted for publication.